

Optimal CO₂ storage management considering safety constraints in multi-stakeholder multi-site CCS projects: a game theoretic perspective

Jungang Chen^{a,*}, Seyyed A. Hosseini^a

^a*Bureau of Economic Geology, Jackson School of Geosciences,
University of Texas at Austin, Austin, TX, 78758, USA*

Abstract

Carbon capture and storage (CCS) projects typically involve a diverse array of *stakeholders* or *players* from public, private, and regulatory sectors, each with different objectives and responsibilities. Given the complexity, scale, and long-term nature of CCS operations, determining whether individual stakeholders can independently maximize their interests—or whether collaborative coalition agreements are needed—remains a central question for effective CCS project planning and management.

CCS projects are often implemented in geologically connected sites, where shared geological features such as pressure space and reservoir pore capacity can lead to competitive behavior among stakeholders. Furthermore, CO₂ storage sites are often located in geologically mature basins that previously served as sites for hydrocarbon extraction or wastewater disposal in order to leverage existing infrastructures, which makes unilateral optimization even more complicated and unrealistic.

In this work, we propose a paradigm based on Markov games to quantitatively investigate how different coalition structures affect the goals of stakeholders. We frame this multi-stakeholder multi-site problem as a multi-agent reinforcement learning problem with safety constraints. Our approach enables agents to learn optimal strategies while compliant with safety regulations. We present an example where multiple operators are injecting CO₂ into their respective project areas in a geologically connected basin. To address the high computational cost of repeated simulations of high fidelity models, a

*Corresponding author: jungang.chen@beg.utexas.edu

previously developed surrogate model based on the Embed-to-Control (E2C) framework is employed. Our results demonstrate the effectiveness of proposed framework in addressing optimal management of CO_2 storage when multiple stakeholders with various objectives and goals are involved.

Keywords: Energy Transition, Geological Carbon Storage, Multi-Agent Reinforcement Learning, Safe Reinforcement Learning Applications, Sequential Decision-Making

1. Introduction

1.1. Background

Geological carbon storage (GCS) has emerged as a viable technology in global efforts to mitigate climate change by permanently sequestering carbon dioxide (CO_2) in deep subsurface formations. As part of the broader carbon capture and storage (CCS) strategy, GCS plays a critical role in reducing anthropogenic emissions from industrial sources while enabling continued use of fossil-based infrastructure during the energy transition (Celia et al., 2015; Hosseini et al., 2024). Modern GCS projects are increasingly being implemented at the basin scale, where geological formations span large areas and support long-term operations and large-volume storage (Huang et al., 2014; Birkholzer and Zhou, 2009; Wijaya et al., 2024). These large-scale deployments often involve multiple injection sites, complex monitoring and regulatory requirements, and diverse stakeholder participation. In this context, multi-stakeholder CCS initiatives—where operators, landowners, regulators, and investors interact within geologically connected sites—are becoming increasingly common.

In a multi-stakeholder CCS setting, each stakeholder pursues distinct interests and goals (Bentham et al., 2014). For example, operators typically manage one or more injection/extraction wells with objectives such as maximizing CO_2 storage or financial returns. Landowners focus on maximizing land use value and royalty income, while regulators prioritize long-term safety, pressure containment, and environmental compliance, e.g. Class VI well regulations (U.S. Environmental Protection Agency, 2013; Leng et al., 2024). Although only operators physically interact with the reservoir, interests of all other stakeholders also shape the operational landscape. For instance, regulators may impose safety constraints that limit injection volumes and rates, whereas landowners and operators may both seek to exploit

the available pressure space for maximum economic return. Moreover, the interconnected nature of subsurface dynamics means that one operator’s injection strategy can alter reservoir pressure and plume behavior, influencing the economic and operational outcomes of other operators.

These inter-dependencies pose significant challenges to effective basin-wide coordination. Without a robust decision-making framework that integrates individual or collective objectives with system-wide regulatory constraints, stakeholders may risk adopting locally optimal strategies that undermine collective performance, leading to underutilized reservoir capacity, reduced economic returns, or even regulatory noncompliance. To this end, coordinated multi-agent optimization is essential to balance return, safety, and fairness in basin-scale GCS deployment.

1.2. Challenges of Multi-agent Optimization in GCS

The challenges of optimal management of basin-scale geological carbon storage are multifold, especially when multiple stakeholders with respective goals and interests are involved. On the one hand, high fidelity models that predict the pressure evolution and plume migration are needed to ensure meeting safety constraints. Optimization of this system requires multiple forward evaluations of these models, which becomes infeasible when the computational resources are limited. A remedy to this is employing machine learning-based proxy models to amortize the computation costs (Wang et al., 2024; Gurwicz et al., 2025). On the other hand, the literature on multi-agent optimization for GCS or broader subsurface communities is scarce. Existing literature either only explored multi-objective optimization of one single stakeholder on various CO₂ storage projects (You et al., 2020; Park et al., 2021; Liu et al., 2025) or constrained co-optimization of one single stakeholder (Zou and Durlofsky, 2023; Nguyen et al., 2024; Tang and Durlofsky, 2025). Recently, (Pettersson et al., 2024, 2025) proposed a multi-objective optimization framework that enables coordinated CO₂ injection strategies among multiple agents in basin-scale carbon storage projects. While this approach facilitates joint optimization, it assumes the presence of a single centralized decision maker who assigns operational strategies to all agents. In doing so, the solution selection may inherently prioritize certain objectives over others—for instance, granting more weight to one agent’s goal. This centralized assumption overlooks the reality that, in practice, each agent seeks to maximize its own returns, therefore limiting the framework’s applicability to competitive multi-operator environments, where decision-making

is inherently decentralized and driven by individual objectives.

1.3. Constrained Markov Game (CMG) and Safe Multi-agent Reinforcement Learning (safe MARL)

In addition to the traditional optimization framework, which based on gradient-based or evolutionary algorithms, a framework referred to as **constrained Markov game (CMG)** (Altman, 2021) is suitable for constrained optimization and offers real-time optimized solutions when multiple actors are involved. A constrained Markov game extends the Markov game framework by adding safety constraints that all agents must comply with while optimizing their own objectives. In a CMG, the system is represented as a sequential decision-making process defined by states, actions, transitions, and rewards, along with explicit safety constraints that limit feasible actions. Safe multi-agent reinforcement learning provides practical methods to learn policies in such settings, ensuring agents maximize rewards while avoiding constraint violations. The detailed formulation of this approach is presented in section 3 and section 4.

This CMG framework is particularly suited to multi-stakeholder CCS projects, where agents operate under competing objectives and must comply with safety regulations. It enables the development of policies that are not only economically optimal but also taking others' operational actions into account, thereby providing a scalable, adaptive decision-making framework for basin-scale CO₂ storage management.

1.4. Contributions and Paper Organization

The contributions of this study are twofold. First, we develop a safe multi-agent reinforcement learning framework tailored for multi-stakeholder, multi-site CO₂ storage problems when each stakeholder has its own goals and interests. The framework accommodates these divergent interests while ensuring safe operations, and its performance is validated against traditional multi-objective optimization approaches. Second, a reward and penalty model is meticulously designed for CO₂ storage projects, and various coalition structures based on shared rewards and penalties have been investigated to evaluate their impacts on stakeholder objectives and overall system performance.

The paper is organized as follows. Section 2 reviews the subsurface dynamics of GCS projects, including key objectives, operational constraints, and potential coalition strategies among stakeholders. Section 3 introduces

fundamental concepts in reinforcement learning and Markov games, establishing the theoretical basis for our approach. Section 4 presents the proposed methodology and workflow. Section 5 reports the case study results. Finally, the paper concludes with a discussion of key findings and a summary of contributions and directions for future work.

2. Problem Formulation

2.1. Overview of Basin-Scale GCS System

Geological CO₂ storage typically consists of studies and analyses across various scales (Guo et al., 2022; Ni et al., 2021) and involves complex coupled multi-physical processes (Nordbotten and Celia, 2011; Jiang, 2011). Deep saline aquifers have abundant storage potential and are regarded as reliable and feasible storage sites. When CO₂ is compressed and supercritical CO₂ is being injected into deep saline aquifers, a compositional multi-phase system is formed. In our study, we consider a compositional porous flow process where the governing equation of the system can be described as:

$$\frac{\partial}{\partial t} (\phi(\rho_w S_w c_{i,w} + \rho_g S_g c_{i,g})) + \nabla \cdot (c_{i,w} \rho_w \mathbf{v}_w + c_{i,g} \rho_g \mathbf{v}_g) = \sum_{j=1}^n (c_{i,w} \rho_w q_w^j + c_{i,g} \rho_g q_g^j) \quad (1)$$

Where the first term is referred to as **accumulation term**, $\frac{\partial}{\partial t}$ is the time differentiation, ϕ stands for porosity, ρ_α and S_α represent phase density and saturation of phase $\alpha = w, g$ respectively; the second term is referred to as **flux term**, $c_{i,\alpha}$ denotes mole fraction of component i in phase α , \mathbf{v}_α is the volumetric velocity of phase α ; the third term denotes the **source/sink term**, q_α^j denotes the volumetric rate for phase α and well j . \mathbf{v}_α is given by Darcy's law, which reads

$$\mathbf{v}_\alpha = -\mathbf{k} \frac{k_{r\alpha}}{\mu_\alpha} (\nabla p_\alpha + \rho_\alpha g \nabla D) \quad (2)$$

Here k refers to the total permeability; $k_{r\alpha}, \mu_\alpha, p_\alpha$ and ρ_α are the relative permeability, viscosity, pressure, and density of α -phase, respectively. g denotes the gravitational constant.

After spatial and temporal discretizations, the above governing equations that describe the compositional flow in porous media can be reformulated as state-space form:

$$\begin{aligned}x_{t+1} &= f(x_t, u_t) \\ y_{t+1} &= g(x_{t+1}, u_t)\end{aligned}\tag{3}$$

where x denotes the system states, including pressure and CO₂ mole fraction, where the dimension may be too large-tens of thousands to millions, which is infeasible for off-policy RL training.

To address the computational burden of high-fidelity reservoir simulations, we leverage a surrogate reduced-order model based on the Embed-to-Control (E2C) architecture (Watter et al., 2015; Jin et al., 2020; Coutinho et al., 2021; Chen et al., 2024a, 2025b), which captures essential system dynamics while significantly reducing simulation time. Employing the machine learning-based reduced-order model, equation 3 can be approximated as:

$$\begin{aligned}z_t &= Enc(x_t; \varphi) \\ z_{t+1} &= f_z(z_t, u_t; \omega_1) \\ \hat{x}_t &= Dec(z_t; \theta) \\ \hat{y}_{t+1} &= g_z(z_{t+1}, u_t; \omega_2)\end{aligned}\tag{4}$$

where Enc , Dec , f_z and g_z are neural networks parameterized by φ , θ , ω_1 and ω_2 , respectively. These neural networks are trained to minimize the reconstruction, regularization and observation data losses. Prior studies have shown that this proxy model maintains high robustness while achieving desirable accuracy compared to high-fidelity simulations. For further implementation and validation details, readers are referred to (Chen et al., 2024b).

2.2. Stakeholders Objectives and Operational Conflicts

Basin-scale carbon capture and storage (CCS) projects involve a diverse array of stakeholders whose interests, responsibilities, and operational controls are inherently interdependent. Figure 1 illustrates the key actors and their roles in a typical CCS project. At the center of the system are operators, who manage CO₂ injection wells (possibly also some brine extraction wells) and directly interface with the subsurface reservoir. Their primary objectives typically include maximizing CO₂ storage volumes and financial returns through strategic control of injection rates and well operations.

Surrounding the operators are other critical stakeholders who, although not directly interacting with the reservoir, exert significant influence over operational decisions. Landowners lease the surface or subsurface rights necessary for storage operations and seek to maximize land-use value and royalty

income. Regulators serve a regulatory role, issuing permits and enforcing constraints to ensure long-term safety, pressure containment, and environmental compliance. In addition, CO₂ suppliers and pipeline operators play a logistical role by delivering captured CO₂ and ensuring transportation infrastructure reliability.

These stakeholders operate within a shared geologic domain and sometimes have misaligned goals. For instance, while both operators and landowners may favor maximizing pressure space for economic benefit, regulators may impose strict injection limits to prevent caprock fracturing or fluid migration beyond permitted boundaries. Moreover, one operator’s injection strategy can affect reservoir pressure distributions and CO₂ plume migration patterns, potentially undermining neighboring operators’ performance or violating shared safety constraints.

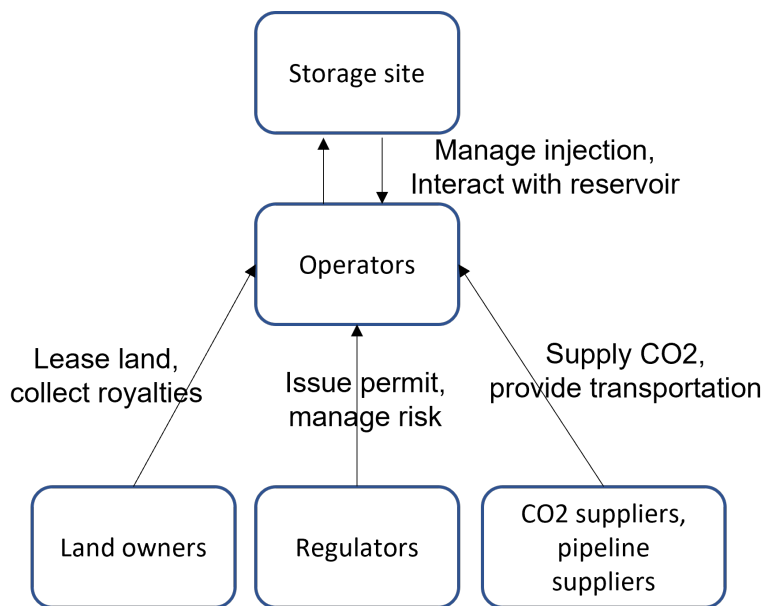


Figure 1: Relations between various stakeholders in a CCS project

2.3. Mathematical Formulation of Objectives

As mentioned earlier, the landlord and operators usually share the common interests, which is to maximize the financial return. Regulator’s interests can translate into safety constraints for the operators. To this end, the following objectives and constraints are proposed.

The financial return is represented as present value (PV), for each agent i , the present value/immediate reward can be defined as:

$$\begin{aligned} \text{PV}_i(u) = & \left(\sum_{j=1}^{N_{\text{inj}}^i} (R_{\text{credit}} - R_{\text{op}}) * q_{t,j}^i(u) \right. \\ & \left. + \sum_{j=1}^{N_{\text{prod}}^i} -R_w * q_{t,w}^i(u) + \sum_{j=1}^{N_{\text{prod}}^i} -R_{\text{CO}_2} * q_{t,g}^i(u) \right) \cdot \Delta t \end{aligned} \quad (5)$$

where the first term represents the revenue from CO₂ credit subtracted by operational costs, the second term indicates the cost to handling the brine water, while the third term is the cost when CO₂ is re-extracted from extraction wells. The parameters R_{credit} , R_{op} , R_w and R_{CO_2} are affected by a variety of economic, policy and technological factors, such as interest rates, carbon incentive policies, brine water handling cost, and etc. To simplify the problem, we assume these parameters remain constant, as shown in table 1. The net present value (NPV) of each agent i is the total cumulative value discounted to current time, which can be expressed as

$$\text{NPV}_i = \sum_{t=1}^{N_t} (\gamma)^t \cdot \text{PV}_i \quad (6)$$

Furthermore, to avoid caprock fracturing and geomechanical risks, each company needs to satisfy the safety constraints, which can be expressed as:

$$p_{\text{grid},i} \leq \alpha_i * p_{\text{frac},i} \quad (7)$$

where $p_{\text{grid},i}$ indicates the pressure at all grid blocks in agent i 's domain, while $p_{\text{frac},i}$ indicates the fracturing pressure for agent i . Note that $p_{\text{grid},i}(u)$ is a function of joint actions by all companies.

2.3.1. Multi-objective optimization formulation

Intuitively, optimal CO₂ storage under multi-stakeholder settings can be formulated as a constrained multi-objective optimization problem, where the objective is to maximize all companies' NPVs while adhering to the pressure constraints. The constrained multi-objective optimization problem can be

formulated as:

$$\begin{aligned}
 \max_u \quad & \{\text{NPV}_1(u), \text{NPV}_2(u), \dots, \text{NPV}_n(u)\} \\
 \text{s.t.} \quad & u_{\min} \leq u \leq u_{\max}, \\
 & p_{grid,i}(u) \leq \alpha * p_{frac,i}, i = 1, 2, \dots, n \\
 & x_{t+1} = f(x_t, u_t), \\
 & y_{t+1} = g(x_{t+1}, u_t),
 \end{aligned} \tag{8}$$

where NPV_i indicates the NPV of agent i , and the decisions u are bounded by operational limits, pressure constraints, and the governing system transition dynamics.

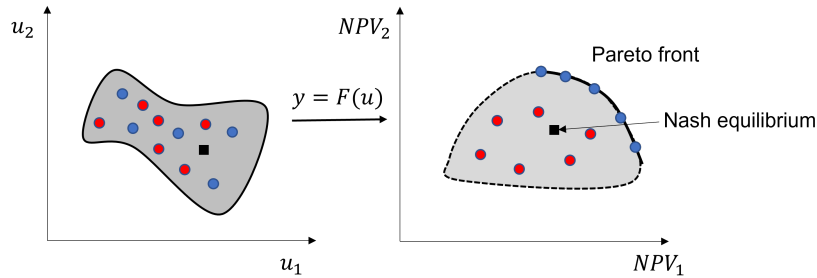


Figure 2: Sketch plot of MOO with two decision variable and two objectives. The gray areas represents the feasible decision and solution space. The blue dots in the objective space represent non-dominated solutions forming the Pareto front: no point on this frontier can be improved in one objective (agent’s reward) without hurting another. The black square indicates a Nash Equilibrium: a point where neither agent can improve their individual reward by unilaterally deviating. Adapted from (Pereira et al., 2022)

Traditionally, MOO problems are addressed using evolutionary algorithms to obtain a Pareto front 2, which provides a spectrum of optimal trade-offs for decision-making. One widely used method is the Non-dominated Sorting Genetic Algorithm II (NSGA-II) (Deb and Jain, 2013), implemented here using the PyMOO framework (Blank and Deb, 2020). In this approach, the algorithm iteratively evolves a population of solutions to converge toward the Pareto-optimal set. Each point on the Pareto front represents a trade-off where no objective can be improved without degrading another. This front can be used for post-optimization solution selection, typically choosing a “knee point” or preference-driven solution.

Despite its effectiveness, the conventional MOO framework may not fully capture the operational realities of CCS projects, as it assumes a single cen-

tralized decision maker with complete knowledge of basin-scale reservoir conditions, inter-well interactions, and the operational strategies of all stakeholders. In practice, CCS operations often involve multiple independent operators, each with limited information and potentially competing interests, making such centralized control unrealistic. Furthermore, while CMOO yields a Pareto front, the resulting solutions often reflect inherent preferences toward certain objectives, which may advantage specific stakeholders. In real-world field operations, post-hoc optimization is rarely feasible due to regulatory, contractual, and operational constraints. These limitations reduce the representativeness of traditional CMOO in modeling actual multi-operator CCS decision-making environments.

2.3.2. Multi-agent reinforcement learning formulation

To address the inherent interdependencies and competing objectives in multi-stakeholder geological carbon storage (GCS), we reformulate the optimization problem as a constrained Markov game as illustrated in Figure 4. In this framework, each operator is represented as an autonomous agent that interacts with the shared reservoir environment while pursuing its individual economic goals subject to safety constraints. The goal of each agent is to maximize its expected discounted cumulative reward:

$$J_i(\pi_1, \dots, \pi_n) = \mathbb{E} \left[\sum_{t=0}^{\infty} \gamma^t r_t^i \right],$$

where π_i denotes the policy of agent i .

Each agent i is associated with a cost/penalty function c_t^i , representing violations of operational safety thresholds (e.g., pore pressure exceeding allowable threshold pressure). The optimization objective thus becomes:

$$\max_{\pi_i} J_i(\pi) = \mathbb{E} \left[\sum_{t=0}^{\infty} \gamma^t r_t^i \right], \quad \text{s.t.} \quad \mathbb{E} \left[\sum_{t=0}^{\infty} \gamma^t c_t^i \right] \leq d_i, \quad \forall i,$$

where d_i denotes the maximum allowable cumulative violation for agent i . More details of this formulation has been presented in section 3.3.

3. Preliminaries

3.1. Deep Reinforcement Learning (DRL)

Deep Reinforcement Learning (DRL) is a branch of machine learning designed for sequential decision-making problems where labeled training data

are unavailable and agents must learn optimal behaviors through repeated interactions with the environment. DRL has registered tremendous success in solving various sequential decision-making problems, including but not limited to: robotics control and maneuver (Kober et al., 2013; Li et al., 2024; Yu et al., 2025a), mechanical system design (Chen et al., 2025a), large language models (Havrilla et al.) and so on. A DRL framework is typically formalized as a Markov Decision Process (MDP) (Figure 3 (a)), in which an agent observes the current state s , selects an action a , and receives a corresponding reward r . The objective is to learn a policy that maximizes the cumulative expected reward over a defined time horizon.

A standard **Markov Decision Process (MDP)** is defined by the tuple

$$\langle \mathcal{S}, \mathcal{A}, \mathbb{T}, r, \gamma \rangle,$$

where:

- \mathcal{S} is the set of states,
- \mathcal{A} is the set of actions,
- $\mathbb{T}(s' | s, a)$ is the transition function to state s' given state s and action a , note that for stochastic processes, it's represented by a transition probability function $\mathbb{P}(s' | s, a)$,
- $R(s, a)$ is the immediate reward,
- $\gamma \in [0, 1)$ is the discount factor.

At each time step t , the agent observes $s_t \in \mathcal{S}$, selects an action $a_t \in \mathcal{A}$ based on a policy $\pi(a | s)$, and receives reward r_t from the environment. The goal is to maximize the **expected cumulative discounted return** over the defined time horizon T :

$$J(\pi) = \mathbb{E}_\pi \left[\sum_{t=0}^T \gamma^t r_t \right] \quad (9)$$

3.2. Multi-Agent Reinforcement Learning (MARL)

When multiple agents interact within the same environment, it becomes a Multi-Agent Reinforcement Learning (MARL) problem (Tampuu et al., 2017; Canese et al., 2021), which is often formulated as a Markov game as

in Figure 3 (b) (Wang et al., 2022). In MARL, each agent receives observations o_i , takes actions a_i , and obtains rewards r_i , while the environment evolves according to the joint actions $[a_1, \dots, a_i, \dots, a_n]$ of all agents. Agents may cooperate, compete, or operate under mixed motives. Cooperation aims to maximize a shared reward, while competitive agents pursue individual objectives, particularly zero-sum objectives. This structure makes MARL well-suited for modeling multi-stakeholder carbon storage projects, where operators, landowners, and regulators pursue distinct but interconnected goals.

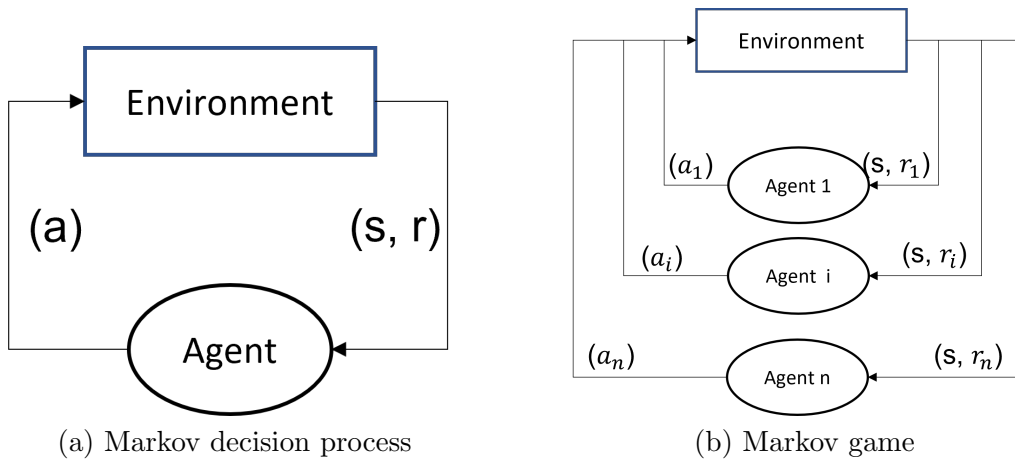


Figure 3: Schematic diagrams of (a) Markov decision process and (b) Markov game, which correspond to the frameworks for (a) single- and (b) multi-agent RL, respectively. Adapted from (Zhang et al., 2021)

In a **Markov game** setting with n agents, the framework is defined as

$$\langle n, \mathcal{S}, \{\mathcal{A}_i\}_{i=1}^n, \mathbb{T}, \{r_i\}_{i=1}^n, \gamma \rangle,$$

where each agent $i \in \{1, \dots, n\}$ has:

- an action space \mathcal{A}_i ,
- a reward function $r_i(s, a_1, \dots, a_n)$,
- a policy $\pi_i(a_i | s)$.

The environment transitions according to the joint action $a = (a_1, \dots, a_n)$:

$$s_{t+1} \sim \mathbb{T}(\cdot | s_t, a_1^t, \dots, a_n^t). \quad (10)$$

In a multi-stakeholder CCS setting, the transition function should comply with subsurface dynamics and can be approximated by a surrogate model as in equation 4. The objective of each agent in MARL framework is to maximize its own expected return:

$$J_i(\pi_1, \dots, \pi_n) = \mathbb{E} \left[\sum_{t=0}^T \gamma^t r_i^t \right] \quad (11)$$

3.3. Multi-Agent Reinforcement Learning (MARL) with Safety Constraints

Conventional MARL does not explicitly account for safety, which is critical in domains where safety is of paramount importance. To address this, safe reinforcement learning (Achiam et al., 2017; Gu et al., 2024; Zheng and Gu, 2024) extends MARL by integrating safety constraints into the decision-making process (Figure 4). Each agent receives not only **rewards** r_i but also **penalties or costs** c_i when actions or resulting system states violate predefined safety thresholds. This constrained Markov game (Altman, 2021) formulation restricts agents to a feasible action space that ensures compliance with operational and regulatory safety requirements – in the case of CO₂ storage, limiting reservoir pressure to prevent caprock fracturing. By embedding safety directly into the learning process, this framework ensures that optimal strategies are not only economically beneficial but also operationally viable and environmentally secure.

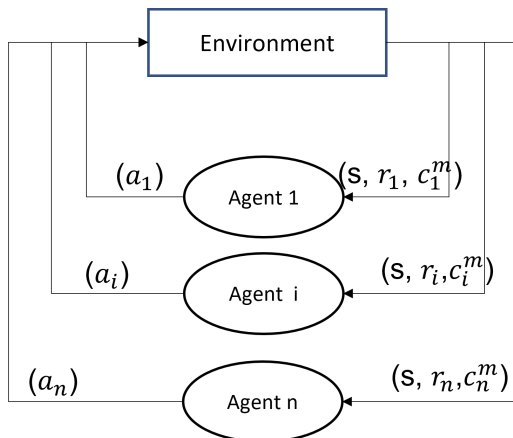


Figure 4: Schematic diagrams of constrained Markov game, which correspond to multi-agent RL with safety constraints. Note that for every agent, there can be m constraints, for simplicity, we assume there is only one constraint when $m = 1$.

A safe multi-agent reinforcement learning framework tailored for GCS is displayed in 5. Each operator/agent is interacting with the subsurface environment and receiving reward r_i and cost c_i at each timestep. Based on the observation o_i , each operator chooses their own well control strategy a_i and the joint actions of all operators a_1, a_2, \dots, a_n drive the current environment state s^t to next environment state s^{t+1} .

To incorporate **safety considerations**, the Markov game is extended into a **Constrained Markov Game (CMG)**:

$$\langle n, \mathcal{S}, \{\mathcal{A}_i\}_{i=1}^n, \mathbb{T}, \{r_i\}_{i=1}^n, \{c_i\}_{i=1}^n, \gamma \rangle,$$

where each agent additionally has a cost function $c_i(s, a)$ representing safety violations (e.g., exceeding reservoir pressure limits). Each agent now optimizes:

$$\max_{\pi_i} J_i(\pi) = \mathbb{E} \left[\sum_{t=0}^{\infty} \gamma^t r_i^t \right] \quad (12)$$

subject to the **safety constraint**:

$$\mathbb{E} \left[\sum_{t=0}^{\infty} \gamma^t c_i^t \right] \leq d_i, \quad \forall i \quad (13)$$

where d_i is the allowable safety threshold for agent i .

A common approach to solve this problem uses **Lagrangian relaxation**, where the objective is reformulated as:

$$\mathcal{L}_i(\pi, \lambda_i) = J_i(\pi) + \lambda_i \left(\mathbb{E} \left[\sum_{t=0}^{\infty} \gamma^t c_i^t \right] - d_i \right), \quad (14)$$

with $\lambda_i \geq 0$ being the Lagrange multiplier balancing reward maximization and constraint enforcement. This coefficient is dynamically updated to penalize constraint violations.

4. Methodologies

4.1. Safe Multi-Agent DDPG (MADDPG) for GCS

To ensure each operator injects safely while maximizing potentially competing objectives in basin-scale CCS, we adopt the Multi-Agent Deep Deterministic Policy Gradient (MADDPG) framework (Lowe et al., 2017). This

framework employs centralized training with decentralized execution to enable multiple operators—modeled as agents—to learn coordinated, well-control policies.

In this setup, each agent i has its own actor–critic network. The deterministic actor $\mu_{\theta_i}(o_i)$ maps the agent’s local observation (e.g., pressures, plume size) to continuous control actions (e.g., injection/extraction rates, bottom-hole pressures). During training, a centralized critic $Q_i^r(s, a_1, \dots, a_N)$ evaluates the joint state–action space, leveraging observations o_i and actions a_i from all agents to mitigate non-stationarity and provide informative gradients. In execution, however, each agent relies solely on its actor network and local observations, maintaining a fully decentralized decision-making process.

To enforce safety constraints, we extend MADDPG with *Lagrangian relaxation*. Alongside the reward critic Q_i^r , a cost critic Q_i^c estimates expected constraint violations (e.g., grid-cell pressures exceeding threshold pressure). The actor for agent i is trained using the Lagrangian objective:

$$\mathcal{L}(\pi_i) = \mathbb{E} \left[- Q_i^r(s, a) + \lambda_i Q_i^c(s, a) \right], \quad (15)$$

where $\lambda_i \geq 0$ is a non-negative weight that controls how strongly safety violations are penalized. It is automatically adjusted during training—if an agent is breaking the safety limit too often, λ_i increases to apply more penalty. The critics are learned through temporal-difference (TD) regression with experience replay and target networks; the actors are updated via deterministic policy gradients; and target networks are soft-updated to stabilize learning. The detailed training and execution scheme was visualized in 15 and the algorithm is shown in 1. This approach yields policies that *maximize economic return while ensuring pressure safety*, aligning directly with our constrained Markov game formulation for multi-stakeholder CCS.

4.2. Adaptations for GCS Optimization

The standard MADDPG framework is adapted to account for the unique features of CCS operations:

- **Reduced-order surrogate modeling:** A machine learning-based proxy, built on the Embed-to-Control (E2C) framework, is employed to approximate high-dimensional reservoir dynamics. This significantly reduces computational overhead while preserving accuracy.

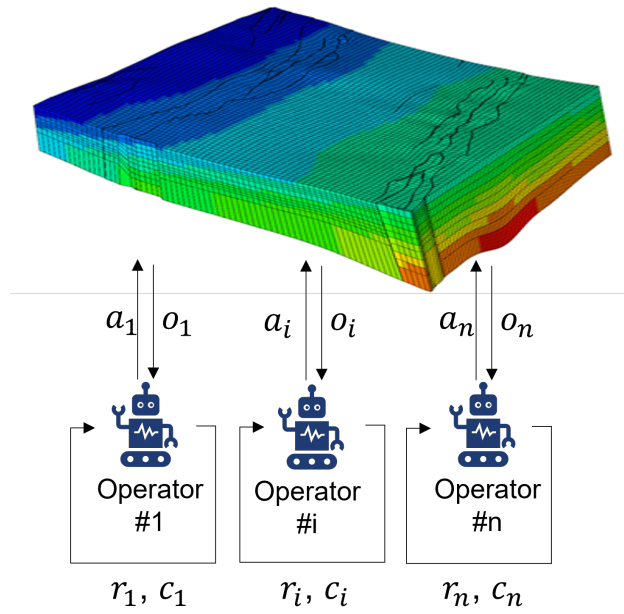


Figure 5: A safe multi-agent reinforcement learning framework tailored for multi-stakeholder CCS projects. Each agent/operator is interacting with subsurface dynamical environment, receiving immediate reward (defined by present values) and penalty (proportional to number of gridblocks that exceed the threshold pressure) and driving the environment to next state.

- **Constraint-aware learning:** Safety constraints are integrated via cost critics and Lagrangian multipliers, ensuring that pore pressure at well locations or each grid cell remains below the allowable threshold pressure ($p_{\text{grid}, i} \leq \alpha p_{\text{frac}, i}$).

4.3. Reward and Penalty Modeling for Geological CO₂ storage

In reinforcement learning, a reward model defines the feedback an agent receives for its actions, signaling which behaviors are beneficial and guiding the agent toward desired outcomes (Yu et al., 2025b; Arora and Doshi, 2021). In safe reinforcement learning, this is complemented by a penalty model, which assigns negative feedback when actions violate safety constraints. Together, reward and penalty models ensure that agents not only maximize designated performance but also operate within required safety and risk boundaries. In multi-agent reinforcement learning (MARL) for geological CO₂ storage (GCS), rewards and penalties must capture the trade-offs between economic returns and regulatory compliance, while accounting for the dynamic, time-dependent nature of subsurface processes.

Common MARL frameworks classify reward structures into three categories: fully competitive, fully cooperative, or mixed competitive-cooperative. However, GCS presents added complexity due to evolving subsurface conditions. At early injection stages, when pressure space is abundant, agents may independently maximize their own net present values (NPVs) without adversely affecting others. At later stages, as pore pressure space becomes constrained, one operator’s increased injection may reduce the feasible capacity of others, introducing significant interdependence and potential conflicts.

To address these challenges, we adopt coalition structures inspired by game theory, enabling flexible combinations of cooperative and competitive behaviors. Coalition structures are enumerated using Bell numbers, allowing evaluation of all possible collaborative configurations. In our case study with three operators (A, B, and C), two primary coalition structure are considered: fully cooperative where all companies act collectively to maximize the total net present value (NPV) of the project, and fully competitive where each company independently seeks to maximize its own NPV without regard for the others. This framework allows us to capture a wide spectrum of strategic behaviors, from joint optimization for mutual benefit to self-interested competition. Based on these coalition types, distinct reward and penalty structures are defined to reflect the corresponding operational incentives and constraints.:

- **{A} v.s {B} v.s {C} setting:** Each agent i maximizes its own net present value (NPV_i), which is cumulative reward over the whole injection period, defined as:

$$NPV_i = \sum_{t=1}^T \gamma^t \cdot PV_i(t) = \sum_{t=1}^T \gamma^t \cdot r_i(t), \quad (16)$$

where $PV_i(t)$ accounts for tax credits and operational costs associated with CO₂ storage and brine handling.

- **{A & B & C} setting:** Agents A, B and C form coalitions to maximize the team reward, defined as the sum of NPVs across coalition members.

$$NPV_i = \sum_{i \in \{A, B, C\}} \sum_{t=1}^T \gamma^t \cdot r_i(t), \quad (17)$$

This incentivizes coordinated well controls and pressure management strategies that improve collective outcomes while maintaining safety.

In the meanwhile, we consider two structures for the penalty model, the first structure only considers imposing penalty when the pore pressure of the injection well grid block exceed the threshold pressure

$$c_i(t) = 5000 \cdot \sum_{g \in \mathcal{G}_{well,i}} \mathbf{1}(p_g^t > p_{threshold}), \quad (18)$$

while the second structure considers a region-wide penalty, defined as:

$$c_i(t) = 50 \cdot \sum_{g \in \mathcal{G}_i} \mathbf{1}(p_g^t > p_{threshold}), \quad (19)$$

In this formulation, c_i^t denotes the penalty incurred by agent i at time step t . The set \mathcal{G}_i represents all grid blocks within company i 's project area, and p_g^t is the pressure in grid block g at time t . The indicator function $\mathbf{1}(p_g^t > p_{i,th})$ returns 1 if the pressure in grid block g exceeds the threshold pressure $p_{i,th}$ assigned to agent i , and 0 otherwise. Thus, the summation counts the total number of violating grid blocks, which is then multiplied by a fixed penalty factor of 50 (50 is selected in a way that the penalty value is of same magnitude of the reward in order for good training practice) to determine the agent's cost at that time step.

This penalty is imposed to train the constrained MADDPG to restrict the actions to feasible solutions:

$$\sum_{t=1}^T \gamma^t \cdot c_i(t) \leq d_i$$

d_i is the penalty threshold, in this experiment, because the pressure constraints are strictly imposed, d_i is set to be 0.0.

This coalition-based reward structuring reflects realistic CCS scenarios, where some stakeholders may choose to collaborate for shared economic and safety benefits, while others pursue individual interests. By embedding coalition flexibility within the MARL framework, we capture the dynamic interplay between cooperation and competition inherent to multi-stakeholder CCS projects.

4.4. Overall Workflow

The overall workflow begins with initializing both the surrogate reservoir model and the multi-agent learning networks. During the training phase, each agent interacts with the reduced-order reservoir environment, generating state-action trajectories that include both reward and penalty signals. These interactions reflect the operational decisions of individual stakeholders and their resulting economic outcomes and constraint violations.

All generated trajectories are stored in a replay buffer, from which mini-batches are sampled to update the actor and critic networks through gradient-based optimization. In parallel, Lagrangian multipliers are updated iteratively to enforce the defined safety constraints, adapting dynamically to the observed level of constraint violations. This coupled update process ensures that the learned policies not only maximize economic returns but also remain compliant with operational safety requirements.

Upon convergence, the trained policies are deployed in a decentralized manner, where each operator controls its own wells exclusively based on local observations without access to global state information. This structure mirrors realistic CCS operational settings, where information sharing between companies may be limited or restricted. The complete implementation of this learning and control process is formalized in Algorithm 1, which integrates the reward and penalty critics, policy updates, and Lagrangian dual optimization into a unified safe multi-agent decision-making framework.

5. Case Study and Results

5.1. Description of Reservoir and Model Setup

The proposed framework is implemented in a synthetic reservoir where the dimension spans $44\text{km} \times 12.8\text{km} \times 0.2\text{km}$ in x, y and z directions. With a depth of 4,000 m and an assumed fracture gradient of 17.0 kPa/m, the fracture pressure p_{frac} is set to be 68,000 kPa. For safe CO₂ injection, the pore pressure must remain below the fracturing pressure, expressed as:

$$p_{\text{grid}} \leq \alpha p_{\text{frac}},$$

where $0.0 < \alpha < 1.0$ reflects site-specific risk tolerance. In this study, α also accounts for the $\sim 3\%$ prediction error between the reduced-order proxy model and the high-fidelity model. The permeability distribution for the basin is shown in Figure 6.

We consider three companies (A, B, and C) operating in non-overlapping regions of the basin (as indicated in the shaded area in 6), each managing a different number of injection wells. To reflect varying risk tolerances, the maximum allowable pore pressure for each company is set to:

$$p_{\text{threshold},i} = \alpha_i p_{\text{frac}} = \begin{cases} 65,000 \text{ kPa}, & i = A, \\ 55,000 \text{ kPa}, & i = B, \\ 55,000 \text{ kPa}, & i = C. \end{cases}$$

The initial reservoir pressure p_{init} is 20,000 kPa. All injection wells are constrained to operate between a minimum rate of 0.5 MMTon/year and a maximum rate of 5.0 MMTon/year:

$$0.5 \text{ MMTon/year} \leq q_{\text{inj}} \leq 5.0 \text{ MMTon/year}.$$

Economic assumptions for revenue and cost calculations are summarized in Table 1, with all companies sharing the same unit revenue and cost structure.

Figure 7 displays well control strategies of all 3 companies for 25 years, while figure 8 presents the corresponding reservoir pressure distribution at the end of injection. In the latter, annotations highlight the maximum grid-block pressures within each company’s leased area at selected injection stages. The results clearly show that under discretionary well control, all three companies operate beyond their allowable pressure thresholds, increasing the risk of caprock fracturing. This exceedance suggests that without coordinated control or imposing safety constraints explicitly, CCS operations may compromise long-term reservoir integrity and storage security.

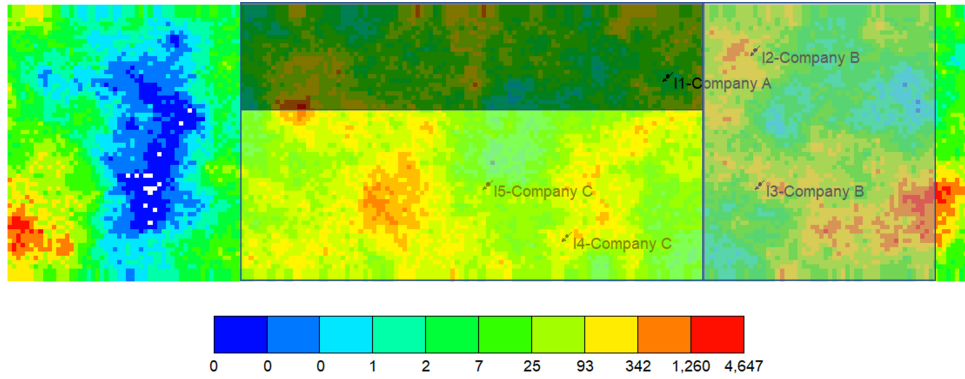


Figure 6: Permeability map (in milliDarcy) of the synthetic basin area. Company A, B and C are operating different numbers of injection/extraction wells. The shadowed area indicating the leased project area of each company.

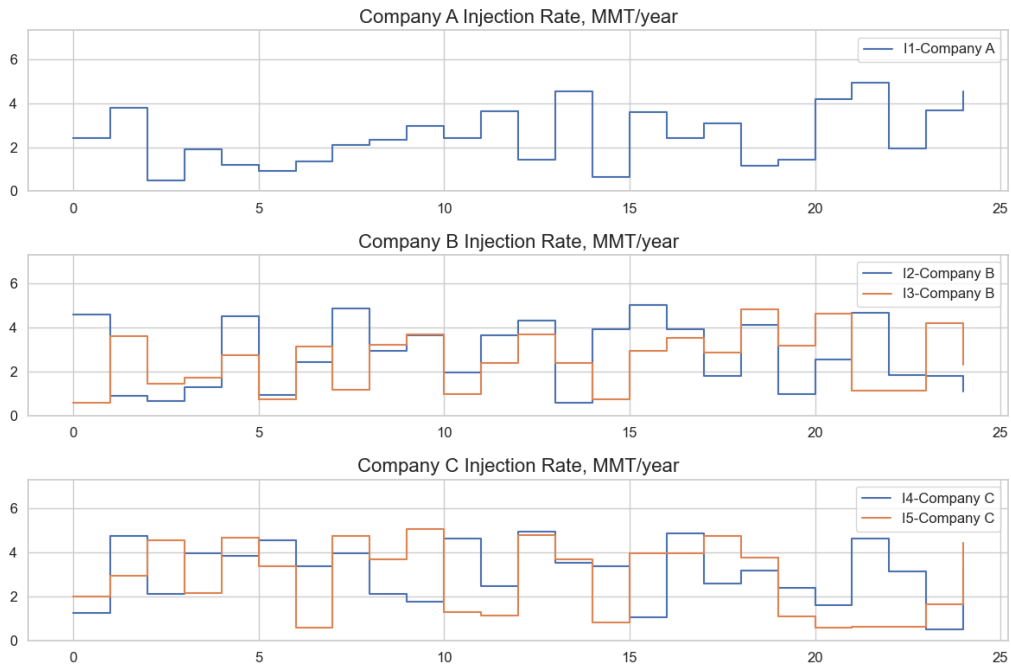


Figure 7: Random well control strategies employed by all companies. The x axis indicates the injection time in years.

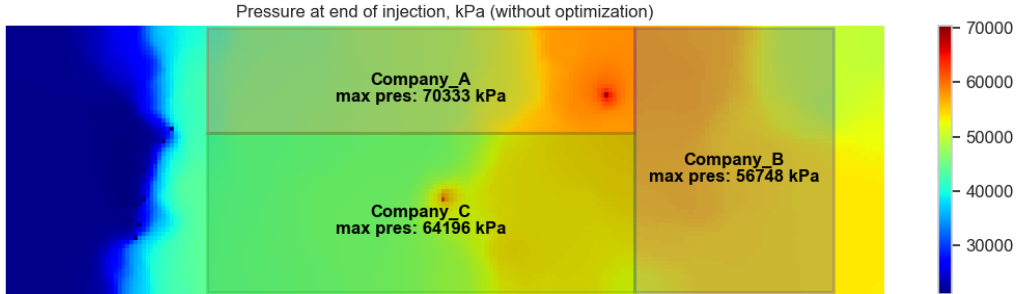


Figure 8: Pressure map at the end of injection if using arbitrary well control strategies in figure 7.

Table 1: CCS project revenues and costs

Revenues/costs	Value
Tax credit (R_{credit}), \$/ton	85
CO ₂ capture, transportation and storage cost (R_{op}), \$/ton	45
Water disposal cost (R_w), \$/ton	30
Discount rate γ	0.95

5.2. Cooperative vs. Competitive from MADDPG

In this subsection, we present the results for scenarios where companies either form a grand coalition to maximize total team NPV (cooperative case) or operate independently without any coalition (competitive case). Figure 9 illustrates the reward and penalty trajectories during training. Initially, both coalition structures adopt aggressive injection strategies, leading to penalties that exceed the predefined safety thresholds. Over time, the penalties decrease and remain below the threshold, indicating compliance with safety constraints. The intermittent pattern of the penalty curve arises from the sparse penalty formulation described in equation 18. While MADDPG does not guarantee a strictly Pareto-optimal policy, we identify the optimal policy as the one achieving the highest team reward while maintaining penalties below the threshold. Figure 10 summarizes the resulting NPVs for both coalition structures, showing that the total team NPV increases from \$6875.34 million in the competitive setting to \$8702.41 million in the cooperative setting. At the company level, company A and C gain substantial benefits from coalition formation, with NPV increases of \$302.33 million and \$1668.91 million, or 14.1% and 95.9% in terms of percentage respectively, compared

to acting alone. In contrast, company B experiences a marginal decrease in NPV. Nevertheless, it would still have an incentive to participate in the coalition if an equitable profit-sharing mechanism were implemented, ensuring mutual benefits across all members.

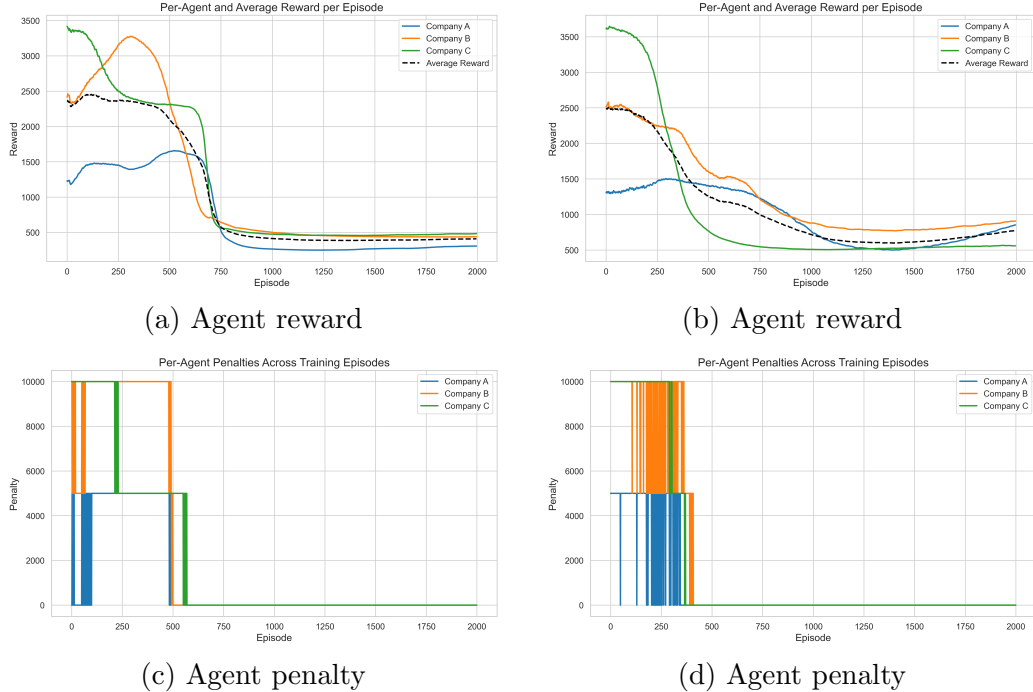


Figure 9: Agent reward and average team reward during training for (a) fully collaborative scenario and (b) fully competitive scenario. And agent penalty during training for (c) fully collaborative scenario and (d) fully competitive scenario. Each episode represents a full simulation run of the CO_2 storage over the defined time horizon. The episode index on the x-axis reflects the progression of training, where early episodes capture exploratory behavior and later episodes reflect increasingly optimized policies.

The proposed framework effectively maintains safe injection pressures across all injection stages, ensuring compliance with injection safety requirements. As illustrated in Figure 11, pressures are monitored at injection well locations for each project area under both fully collaborative and fully competitive scenarios. However, because only point-wise constraints are applied, regional compliance with pressure limits is not guaranteed. This limitation is evident in figure 11 (b), where at the end of injection, the maximum pres-

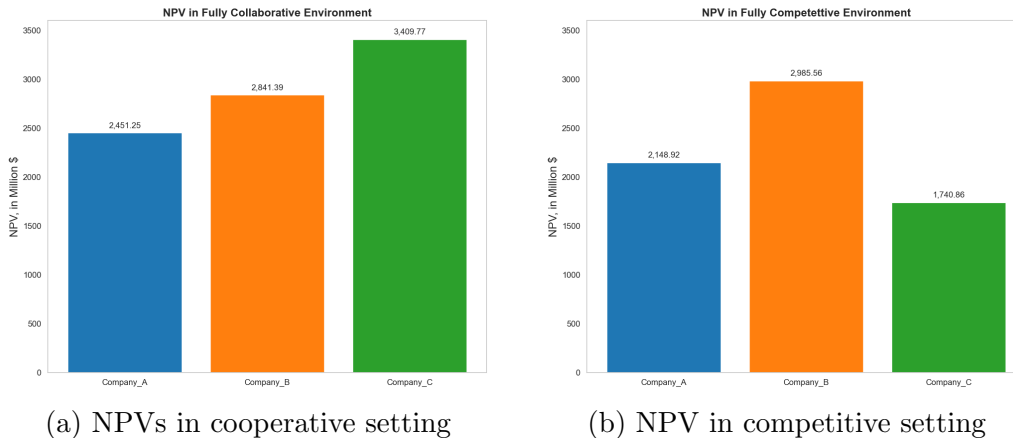


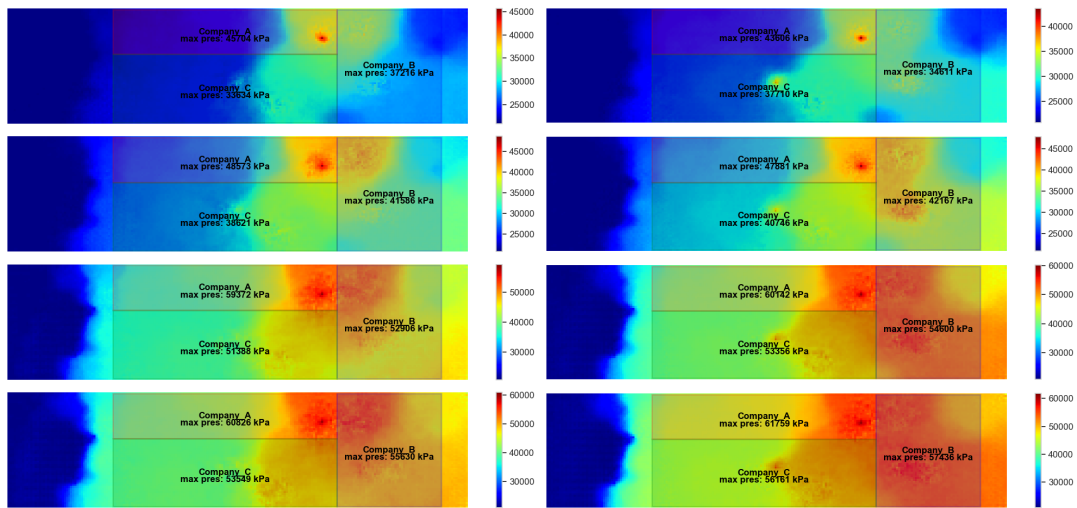
Figure 10: NPV of each company under (a) fully collaborative scenario and (b) fully competitive scenario. The total team NPV from fully collaborative scenario is \$8702.41 Million, while the total NPV from fully competitive case is \$6875.34 Million.

sure in Company B’s area exceeds its threshold of 55,000 kPa due to pressure migration from neighboring regions, particularly from Company A’s area—a phenomenon referred to as pressure trespass (de Figueiredo, 2005). These highlight the necessity of a system-wide penalty model that accounts for interactions across project boundaries, especially in cases where companies operate under different pressure thresholds and risk tolerances.

5.3. Comparison against MOO results

In this subsection, we assess the performance of the proposed CMG framework relative to conventional MOO algorithms. The Pareto front generated by CMOO for the competitive case is illustrated in figure 12, while Table 2 summarizes the NPV results across different coalition structures and methods. In the fully collaborative scenario, safe MADDPG yields the highest total NPV of \$8720.41 M, exceeding MOO’s best collaborative result (\$8544.07 M) by a notable margin. In the fully competitive setting, MADDPG attains a NPV of \$6875.34 M, which is lower than any of MOO’s competitive allocations, this can be explained that MADDPG in a competitive setting becomes not Pareto optimal due to decentralized structure.

From a per-company perspective, MADDPG provides relatively balanced gains without overly favoring one company at the expense of others, while MOO’s preference-based allocations (favoring A, B, or C) can result in dis-



(a) Pressure map at selected injection periods, in kPa (b) Pressure map at selected injection periods, in kPa

Figure 11: Pressure maps at different injection stages $t = 5, 10, 20, 25$ years (from top to bottom) for (a) fully collaborative scenario and (b) fully competitive scenario. The maximum pressure at each leased project area is annotated.

proportionate benefits to a single entity. Although MADDPG does not guarantee Pareto-optimality for all scenarios, its adaptive learning strategies effectively navigate the trade-off between cooperative and competitive objectives. This makes it a robust choice for maximizing system-wide returns while mitigating excessive inequality among stakeholders.

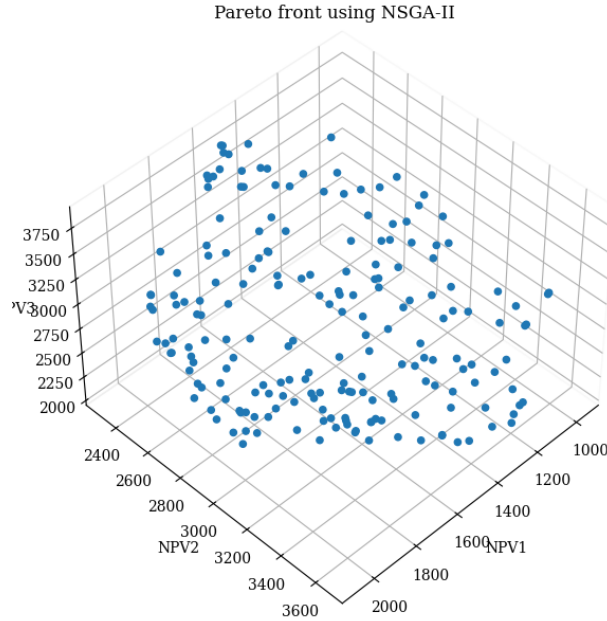


Figure 12: Pareto front obtained using NSGA-II for the fully competitive case. The units are in \$ million.

Table 2: NPV results (million \$) for different methods.

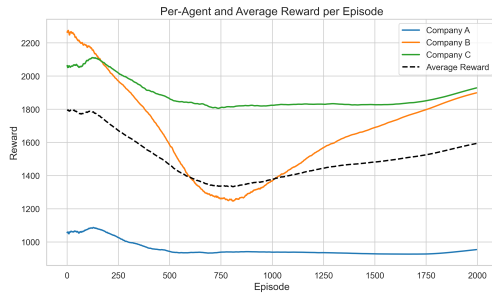
Methods	Company A	Company B	Company C	Total
MADDPG, fully collab	2451.25	2841.39	3409.77	8720.41
MADDPG, fully comp	2148.92	2985.56	1740.86	6875.34
MOO, fully collab	2039.10	3395.51	3109.46	8544.07
MOO, fully comp(knee point)	1482.99	2989.91	3587.52	8060.41
MOO, fully comp(favoring A)	2069.77	2799.95	2661.47	7531.19
MOO, fully comp(favoring B)	1251.45	3654.18	2216.09	7121.72
MOO, fully comp(favoring C)	1544.31	2319.41	3827.17	7690.90

5.4. *Region-wide Penalty Model*

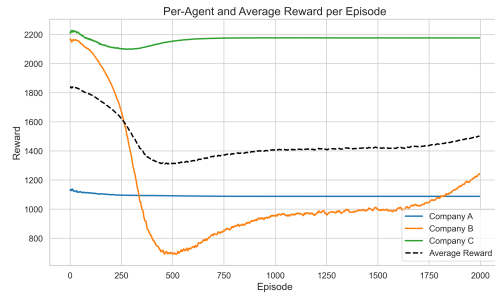
In this subsection, we assess the effectiveness of implementing a region-wide penalty, as formulated in Equation 19, to ensure that safety constraints are satisfied across the entire project area. Unlike the point-wise penalty approach, which focuses only on injection well locations, the region-wide penalty enforces compliance at all spatial locations.

Figure 13 illustrates the evolution of reward and penalty during training. Compared to the point-wise penalty case, the region-wide approach yields a denser penalty profile early in training. Over time, penalties steadily decline and stabilize below the threshold, demonstrating that the learned policies achieve safe operation consistently across all regions.

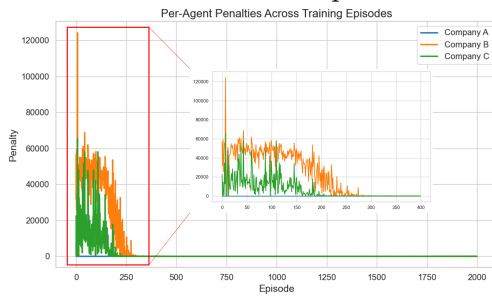
The corresponding pressure maps in Figure 14 confirm that, under both cooperative and competitive scenarios, maximum pore pressures at all injection stages remain below their respective thresholds in every subregion. This highlights not only the robustness of the safe-MADDPG framework but also the value of the region-wide penalty in guiding policy learning toward globally feasible and safe injection strategies, even when multiple agents with potentially conflicting objectives are involved.



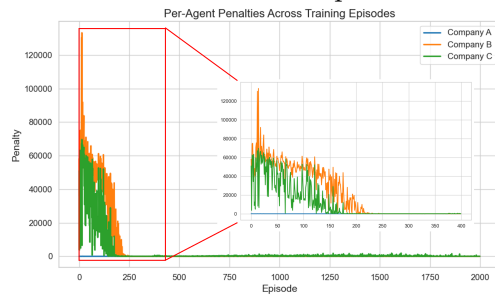
(a) Agent reward when region-wide constraints are imposed



(b) Agent reward when region-wide constraints are imposed

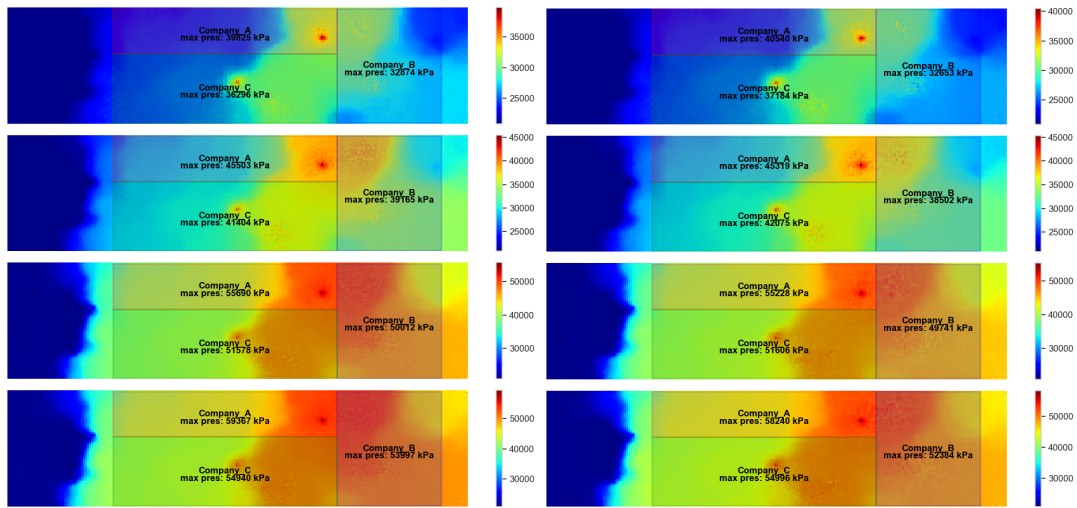


(c) Agent penalty when region-wide constraints are imposed



(d) Agent penalty when region-wide constraints are imposed

Figure 13: Agent reward and average team reward during training when region-wide constraints are imposed for (a) fully collaborative scenario and (b) fully competitive scenario. And agent penalty during training for (c) fully collaborative scenario and (d) fully competitive scenario.



(a) Pressure map at selected injection periods when region-wide constraints are imposed, in kPa

(b) Pressure map at selected injection periods when region-wide constraints are imposed, in kPa

Figure 14: Pressure maps at different injection stages $t = 5, 10, 20, 25$ years (from top to bottom) for (a) fully collaborative scenario and (b) fully competitive scenario. The maximum pressure at each leased project area is annotated. It can be observed that the proposed framework guarantees safe injection at all CCS stages as the maximum pressure at each leased area is less than each company's threshold pressure as described in 5.1.

6. Conclusions

A safe Multi-Agent Deep Deterministic Policy Gradient (MADDPG) framework based on a constrained Markov game has been developed to optimize each stakeholder’s objectives in geological carbon storage (GCS) operations while ensuring compliance with safety constraints. The proposed approach, although not strictly guaranteeing Pareto-optimality, consistently delivers strong performance in both competitive and cooperative scenarios.

In optimal basin-scale CCS management, reward and penalty designs play a central role in maximizing stakeholders’ objectives within safety constraints. In this work, reward models based on fully cooperative and fully competitive settings are discussed. Two penalty model strategies were investigated – point-wise and region-wide – and the results show that applying project-wide constraints is essential to prevent pressure trespassing from one operator’s lease area into another, particularly when operators have varying risk tolerances. This ensures a more equitable and safe operational environment. Overall, the safe MADDPG effectively balances economic objectives with safety requirements, demonstrating its potential as a robust decision-making tool for multi-stakeholder CO_2 storage projects with safety requirements.

In future work, we aim to investigate partially cooperative scenarios, where certain subsets of stakeholders collaborate while simultaneously competing with others. Such mixed cooperation–competition settings better reflect the complexities of real-world coalition agreements in CCS operations. In addition, we plan to develop multi-agent reinforcement learning algorithms with explicit Pareto-optimality guarantees, ensuring that learned strategies achieve efficient trade-offs where no stakeholder’s outcome can be improved without reducing others’. These advancements will enhance the framework’s applicability to more realistic operational contexts.

Acknowledgments

We are grateful to the Gulf Coast Carbon Center at UT Austin and its sponsors for funding this work. We thank Sean Avitt for providing the Wilcox Group geomodel in Figure 5. Thanks also go to Computer Modeling Group Ltd. for providing the simulation software.

Data Availability

The code will be made available at https://github.com/jungangc/CCS_MARL once published.

References

- Achiam, J., Held, D., Tamar, A., Abbeel, P., 2017. Constrained policy optimization, in: International conference on machine learning, PMLR. pp. 22–31.
- Altman, E., 2021. Constrained Markov decision processes. Routledge.
- Arora, S., Doshi, P., 2021. A survey of inverse reinforcement learning: Challenges, methods and progress. *Artificial Intelligence* 297, 103500.
- Bentham, M., Pearce, J., Kirk, K., Hovorka, S., van Gessel, S., Pegler, B., Neades, S., Dixon, T., 2014. Managing co2 storage resources in a mature ccs future. *Energy Procedia* 63, 5310–5324.
- Birkholzer, J.T., Zhou, Q., 2009. Basin-scale hydrogeologic impacts of co2 storage: Capacity and regulatory implications. *International Journal of Greenhouse Gas Control* 3, 745–756.
- Blank, J., Deb, K., 2020. pymoo: Multi-objective optimization in python. *IEEE Access* 8, 89497–89509.
- Canese, L., Cardarilli, G.C., Di Nunzio, L., Fazzolari, R., Giardino, D., Re, M., Spanò, S., 2021. Multi-agent reinforcement learning: A review of challenges and applications. *Applied Sciences* 11, 4948.
- Celia, M.A., Bachu, S., Nordbotten, J.M., Bandilla, K.W., 2015. Status of co2 storage in deep saline aquifers with emphasis on modeling approaches and practical simulations. *Water Resources Research* 51, 6846–6892.
- Chen, J., Gidlin, E., Killough, J., 2024a. Advancing proxy modeling in reservoir simulation: A multi-step embed to control approach, in: SPE Annual Technical Conference and Exhibition?, SPE. p. D021S023R006.

- Chen, J., Gildin, E., Kompantsev, G., 2024b. Optimization of pressure management strategies for geological co2 storage using surrogate model-based reinforcement learning. *International Journal of Greenhouse Gas Control* 138, 104262.
- Chen, S., Bayrak, A.E., Sha, Z., 2025a. A cost-aware multi-agent system for black-box design space exploration. *Journal of Mechanical Design* 147, 011703.
- Chen, Y., Nguyen, Q.M., Abdulkareem, U., Onur, M., Alpak, F.O., 2025b. Application of embed-to-control observe deep-learning-based reservoir surrogate in co2 storage monitoring and multi-objective optimization, in: *SPE Reservoir Simulation Conference, SPE*. p. D021S008R002.
- Coutinho, E.J.R., Dall’Aqua, M., Gildin, E., 2021. Physics-aware deep-learning-based proxy reservoir simulation model equipped with state and well output prediction. *Frontiers in Applied Mathematics and Statistics* 7, 651178.
- Deb, K., Jain, H., 2013. An evolutionary many-objective optimization algorithm using reference-point-based nondominated sorting approach, part i: solving problems with box constraints. *IEEE transactions on evolutionary computation* 18, 577–601.
- de Figueiredo, M.A., 2005. Property Interests and Liability of Geologic Carbon Dioxide Storage. Special Report. MIT Carbon Sequestration Initiative, Massachusetts Institute of Technology.
- Gu, S., Yang, L., Du, Y., Chen, G., Walter, F., Wang, J., Knoll, A., 2024. A review of safe reinforcement learning: Methods, theories and applications. *IEEE Transactions on Pattern Analysis and Machine Intelligence* .
- Guo, R., Dalton, L., Crandall, D., McClure, J., Wang, H., Li, Z., Chen, C., 2022. Role of heterogeneous surface wettability on dynamic immiscible displacement, capillary pressure, and relative permeability in a co2-water-rock system. *Advances in Water Resources* 165, 104226.
- Gurwicz, A., Chen, J., Gutman, D., Gildin, E., 2025. Assessing risk in long-term co2 storage under uncertainty via survival analysis-based surrogates. *SPE Journal* 30, 2837–2854.

- Havrilla, A., Du, Y., Raparthy, S.C., Nalmpantis, C., Dwivedi-Yu, J., Hambro, E., Sukhbaatar, S., Raileanu, R., . Teaching large language models to reason with reinforcement learning, in: AI for Math Workshop@ ICML 2024.
- Hosseini, S.A., Ershadnia, R., Lun, L., Morgan, S., Bennett, M., Skrivanos, C., Li, B., Soltanian, M.R., Pawar, R., Hovorka, S.D., 2024. Dynamic modeling of geological carbon storage in aquifers–workflows and practices. *International Journal of Greenhouse Gas Control* 138, 104235.
- Huang, X., Bandilla, K.W., Celia, M.A., Bachu, S., 2014. Basin-scale modeling of co2 storage using models of varying complexity. *International Journal of Greenhouse Gas Control* 20, 73–86.
- Jiang, X., 2011. A review of physical modelling and numerical simulation of long-term geological storage of co2. *Applied Energy* 88, 3557–3566.
- Jin, Z.L., Liu, Y., Durlofsky, L.J., 2020. Deep-learning-based surrogate model for reservoir simulation with time-varying well controls. *Journal of Petroleum Science and Engineering* 192, 107273.
- Kober, J., Bagnell, J.A., Peters, J., 2013. Reinforcement learning in robotics: A survey. *The International Journal of Robotics Research* 32, 1238–1274.
- Leng, J., Bump, A., Hosseini, S.A., Meckel, T.A., Wang, Z., Wang, H., 2024. A comprehensive review of efficient capacity estimation for large-scale co2 geological storage. *Gas Science and Engineering* 126, 205339.
- Li, K., Chen, J., Yu, D., Dajun, T., Qiu, X., Lian, J., Ji, R., Zhang, S., Wan, Z., Sun, B., et al., 2024. Deep reinforcement learning-based obstacle avoidance for robot movement in warehouse environments, in: 2024 IEEE 6th International Conference on Civil Aviation Safety and Information Technology (ICCASIT), IEEE. pp. 342–348.
- Liu, J., Liu, J., Zhu, Y., Sun, W., Zhang, D., Pan, H., 2025. Multi-objective optimization for efficient co2 storage under pressure buildup constraint in saline aquifer. *Applied Energy* 382, 125175.
- Lowe, R., Wu, Y.I., Tamar, A., Harb, J., Pieter Abbeel, O., Mordatch, I., 2017. Multi-agent actor-critic for mixed cooperative-competitive environments. *Advances in neural information processing systems* 30.

- Nguyen, Q.M., Onur, M., Alpak, F.O., 2024. Multi-objective optimization of subsurface co₂ capture, utilization, and storage using sequential quadratic programming with stochastic gradients. *Computational Geosciences* 28, 195–210.
- Ni, H., Møyner, O., Kurtev, K.D., Benson, S.M., 2021. Quantifying co₂ capillary heterogeneity trapping through macroscopic percolation simulation. *Advances in Water Resources* 155, 103990.
- Nordbotten, J.M., Celia, M.A., 2011. Geological storage of CO₂: modeling approaches for large-scale simulation. John Wiley & Sons.
- Park, C., Oh, J., Jo, S., Jang, I., Lee, K.S., 2021. Multi-objective optimization of co₂ sequestration in heterogeneous saline aquifers under geological uncertainty. *Applied Sciences* 11, 9759.
- Pereira, J.L.J., Oliver, G.A., Francisco, M.B., Cunha Jr, S.S., Gomes, G.F., 2022. A review of multi-objective optimization: methods and algorithms in mechanical engineering problems. *Archives of Computational Methods in Engineering* 29, 2285–2308.
- Pettersson, P., Krumscheid, S., Gasda, S., 2024. Multi-objective optimization for multi-agent injection strategies in subsurface co₂ storage, in: *ECMOR 2024*, European Association of Geoscientists & Engineers. pp. 1–14.
- Pettersson, P., Krumscheid, S., Gasda, S., 2025. Cooperative games defined by multi-objective optimization in competition for subsurface resources. *arXiv preprint arXiv:2502.19987* .
- Tampuu, A., Matiisen, T., Kodelja, D., Kuzovkin, I., Korjus, K., Aru, J., Aru, J., Vicente, R., 2017. Multiagent cooperation and competition with deep reinforcement learning. *PloS one* 12, e0172395.
- Tang, H., Durlofsky, L.J., 2025. Graph network surrogate model for optimizing the placement of horizontal injection wells for co₂ storage. *International Journal of Greenhouse Gas Control* 145, 104404.
- U.S. Environmental Protection Agency, 2013. Underground Injection Control (UIC) Program Class VI Well Area of Review Evaluation and Corrective Action Guidance. Technical Report EPA 816-R-13-005. U.S. Environmental Protection Agency.

- Wang, H., Hosseini, S.A., Tartakovsky, A.M., Leng, J., Fan, M., 2024. A deep learning-based workflow for fast prediction of 3d state variables in geological carbon storage: A dimension reduction approach. *Journal of Hydrology* 636, 131219.
- Wang, J., Hong, Y., Wang, J., Xu, J., Tang, Y., Han, Q.L., Kurths, J., 2022. Cooperative and competitive multi-agent systems: From optimization to games. *IEEE/CAA Journal of Automatica Sinica* 9, 763–783.
- Watter, M., Springenberg, J., Boedecker, J., Riedmiller, M., 2015. Embed to control: A locally linear latent dynamics model for control from raw images. *Advances in neural information processing systems* 28.
- Wijaya, N., Morgan, D., Vikara, D., Grant, T., Cunha, L., Liu, G., 2024. Basin-scale study of co2 storage in stacked sequence of geological formations. *Scientific Reports* 14, 18661.
- You, J., Ampomah, W., Sun, Q., 2020. Development and application of a machine learning based multi-objective optimization workflow for co2-eor projects. *Fuel* 264, 116758.
- Yu, D., Liu, L., Wu, S., Li, K., Wang, C., Xie, J., Chang, R., Wang, Y., Wang, Z., Ji, R., 2025a. Machine learning optimizes the efficiency of picking and packing in automated warehouse robot systems, in: *2025 IEEE International Conference on Electronics, Energy Systems and Power Engineering (EESPE)*, IEEE. pp. 1325–1332.
- Yu, R., Wan, S., Wang, Y., Gao, C.X., Gan, L., Zhang, Z., Zhan, D.C., 2025b. Reward models in deep reinforcement learning: A survey. *arXiv preprint arXiv:2506.15421* .
- Zhang, K., Yang, Z., Başar, T., 2021. Multi-agent reinforcement learning: A selective overview of theories and algorithms. *Handbook of reinforcement learning and control* , 321–384.
- Zheng, Z., Gu, S., 2024. Safe multi-agent reinforcement learning with bilevel optimization in autonomous driving. *IEEE Transactions on Artificial Intelligence* .

Zou, A., Durlinsky, L.J., 2023. Integrated framework for optimization of horizontal/deviated well placement and control for geological co2 storage, in: SPE Reservoir Simulation Conference, SPE. p. D021S010R003.

Appendix

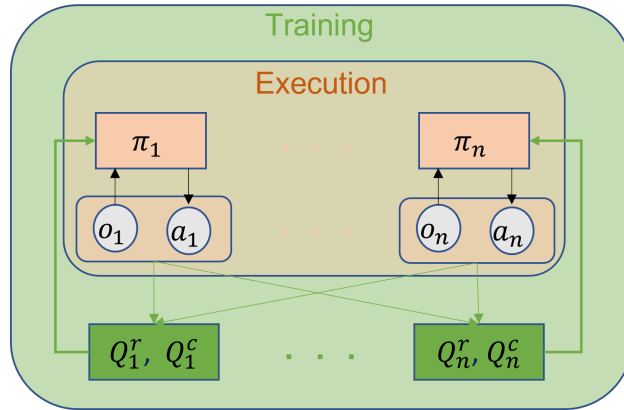
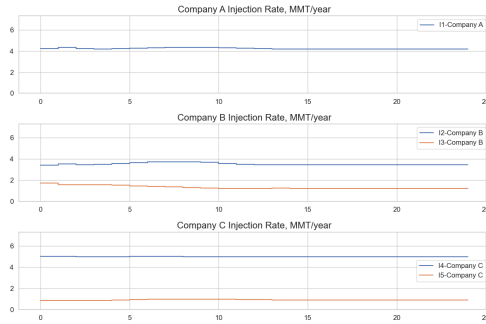
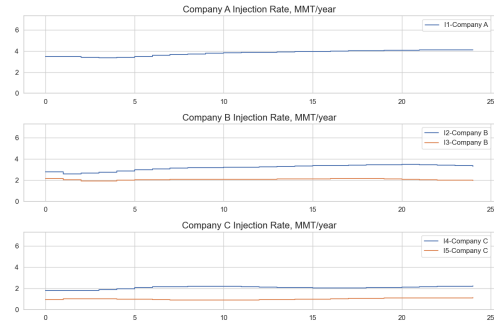


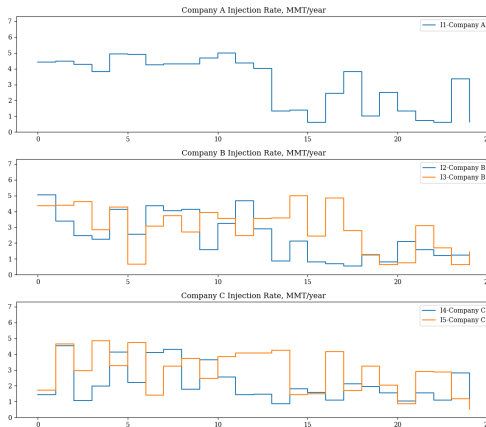
Figure 15: Safe MADDPG with centralized training and decentralized execution (CTDE) (Lowe et al., 2017). Inside the *Execution* box, each agent i selects $a_i = \pi_i(o_i)$ from its local observation. During *Training* (outer box), a reward critic Q_i^r and a cost critic Q_i^c for each agent condition on the joint tuple $(o_{1:n}, a_{1:n})$ and backpropagate gradients to the actors. Safety is enforced via a Lagrangian penalty $-\lambda_i Q_i^c$, with multipliers λ_i updated to penalize constraint violations; at evaluation time only the policies run, while critics (and λ_i updates) are not required.



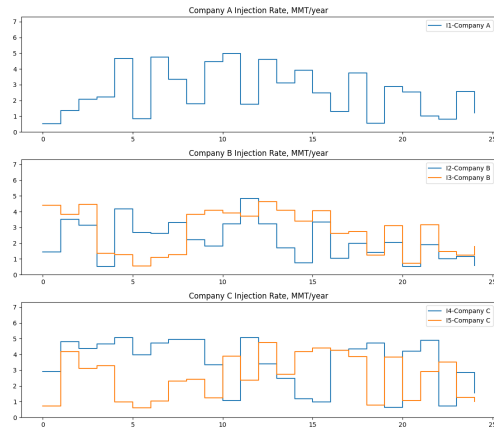
(a) Optimal well injection strategies over 25 years from safe MADDPG



(b) Optimal well injection strategies over 25 years from safe MADDPG



(c) Optimal well injection strategies over 25 years from CMOO



(d) Optimal well injection strategies over 25 years from CMOO

Figure 16: Optimal well injection strategies over 25 years from two approaches (a) fully collaborative scenario and (b) fully competitive scenario (c) fully collaborative scenario and (d) fully competitive scenario.

Algorithm 1 Constrained MADDPG for multi-stakeholder CO₂ management

Require: episodes M , horizon T , discount γ , soft update rate τ , replay buffer \mathcal{D} , exploration noise \mathcal{N} , safety threshold \bar{c} , dual stepsize η_λ , max multiplier λ_{\max} , actor μ_i with parameters θ_i , reward critic Q_i^r with params ϕ_i^r , penalty critic Q_i^c with params ϕ_i^c

- 1: **Initialize:** target networks $\theta'_i \leftarrow \theta_i$, $\phi_i^{r'} \leftarrow \phi_i^r$, $\phi_i^{c'} \leftarrow \phi_i^c$; $\lambda \geq 0$
- 2: **for** episode = 1 to M **do**
- 3: Reset environment; get initial observations o_1, \dots, o_N
- 4: **for** $t = 1$ to T **do**
- 5: **(Act)** For each agent i , select action $a_i \leftarrow \mu_i(o_i) + \mathcal{N}_t$
- 6: Execute joint action $\mathbf{a} = (a_1, \dots, a_N)$; observe reward vector \mathbf{r} , penalty vector \mathbf{c} and next observations \mathbf{o}' according to equations 4, 16–19.
- 7: Store transition $(\mathbf{o}, \mathbf{a}, \mathbf{r}, \mathbf{c}, \mathbf{o}')$ in buffer \mathcal{D} ; set $\mathbf{o} \leftarrow \mathbf{o}'$

- 8: **(Learn)** Sample a minibatch $\{(\mathbf{o}^j, \mathbf{a}^j, \mathbf{r}^j, \mathbf{c}^j, \mathbf{o}'^j)\}_{j=1}^S \sim \mathcal{D}$
- 9: **for** $i = 1$ to N **do** ▷ update per agent
- 10: $y_i^{r,j} \leftarrow r_i^j + \gamma Q_i^{r'}(\mathbf{o}^j, a_1^j, \dots, a_N^j) \Big|_{a_k^j \leftarrow \mu_k^r(o_k^j)}$
- 11: $y_i^{c,j} \leftarrow c_i^j + \gamma Q_i^{c'}(\mathbf{o}^j, a_1^j, \dots, a_N^j) \Big|_{a_k^j \leftarrow \mu_k^c(o_k^j)}$
- 12: Update critics by minimizing

$$\mathcal{L}_i^r(\phi_i^r) = \frac{1}{S} \sum_{j=1}^S \left(y_i^{r,j} - Q_i^r(\mathbf{o}^j, \mathbf{a}^j) \right)^2, \quad \mathcal{L}_i^c(\phi_i^c) = \frac{1}{S} \sum_{j=1}^S \left(y_i^{c,j} - Q_i^c(\mathbf{o}^j, \mathbf{a}^j) \right)^2$$

- 13: Update actors with sampled policy gradient

$$J_i(\theta_i) = \frac{1}{S} \sum_{j=1}^S \left[-Q_i^r(\mathbf{o}^j, a_1^j, \dots, a_N^j) + \lambda Q_i^c(\mathbf{o}^j, a_1^j, \dots, a_N^j) \right] \Big|_{a_k^j \leftarrow \mu_k^r(o_k^j)}$$

- 14: dual update for Lagrange multiplier:

$$\lambda \leftarrow \max\left(0, \lambda + \eta_\lambda \left(\frac{1}{NS} \sum_{i=1}^N \sum_{j=1}^S (Q_i^c - \bar{c}) \right)\right)$$

- 15: **end for**
- 16: **Target soft updates** (for each i):

$$\theta'_i \leftarrow \tau \theta_i + (1 - \tau) \theta'_i, \quad \phi_i^{r'} \leftarrow \tau \phi_i^r + (1 - \tau) \phi_i^{r'}, \quad \phi_i^{c'} \leftarrow \tau \phi_i^c + (1 - \tau) \phi_i^{c'}$$

- 17: **end for**
 - 18: **end for**
-